



Downregulation of Transmembrane protein 40 by miR-138-5p Suppresses Cell Proliferation and Mobility in Clear Cell Renal Cell Carcinoma

Dongcao Liu, Guang Zhou*, Hongbo Shi, Bin Chen, Xiaosong Sun, Xuejun Zhang

Department of Urology, Xiangyang Central Hospital, Affiliated Hospital of Hubei University of Arts and Science, Xiangyang, China

*Corresponding author: Guang Zhou, Department of Urology, Xiangyang Central Hospital, Affiliated Hospital of Hubei University of Arts and Science, No. 136, Jingzhou Street, Xiangcheng, Xiangyang City 441021, Hubei Province, China Tel/Fax: +86-0710-3524509. E-mail: guangZhou_2015@126.com

Background: Clear cell renal cell carcinoma (ccRCC) represents approximately 70% of RCC, as the most frequent histological subtype of RCC. MiR-138-5p, a tumor-related microRNA (miRNA), has been reported to be implicated in the diverse types of human malignancies, but its role in ccRCC remains unclear.

Objective: The study was designed to investigate the functional behaviors and regulatory mechanisms of miR-138-5p in ccRCC.

Materials and Methods: Quantitative real-time PCR and western blotting analyses were performed to determine the expression of miR-138-5p and Transmembrane protein 40 (TMEM40) in ccRCC tissues. Pearson's correlation coefficient was utilized to evaluate the correlation between miR-138-5p and TMEM40 expression. The function of miR-138-5p and TMEM40 in the cell proliferation, migration and invasion of ccRCC cells (786-O and ACHN) was assessed by Cell Counting Kit-8, colony formation, wound healing and transwell assay, respectively. A luciferase reporter assay was performed to confirm the direct binding of miR-138-5p to the target gene TMEM40.

Results: We found the expression of miR-138-5p was significantly down-regulated, while TMEM40 was remarkably up-regulated in ccRCC tissues. TMEM40 expression was discovered to be inversely correlated with miR-138-5p expression in ccRCC tissues. Functional studies demonstrated that miR-138-5p overexpression or TMEM40 knockdown significantly suppressed ccRCC cell proliferation, migration and invasion *in vitro*. Notably, we experimentally confirmed that miR-138-5p directly recognizes the 3'-UTR of the TMEM40 transcript and down-regulated its expression in ccRCC cells.

Conclusions: Taken together, our findings provide the first clues regarding the role of miR-138-5p as a tumor suppressor in ccRCC by directly targeting of TMEM40.

Keywords: Clear Cell Renal Cell Carcinoma, miR-138-5p, TMEM40, Tumor Suppressor

1. Background

Each year, approximately 65,000 new cases of kidney cancers will be diagnosed, and kidney cancer causing 13680 deaths are found in the United States (1). Up to 15%-20% of patients have concurrent lymph node metastasis and a similar proportion are found to have distant metastasis when they were diagnosed with kidney cancer (2). Clear cell renal cell carcinoma (ccRCC) is a highly-lethal subtype of kidney cancer (3). Until now, surgical, stereotactic radiotherapy, chemotherapy, and adjuvant therapy have been advocated as major means to substantially reduce the morbidity of ccRCC. However, the median survival for metastatic patients remains poor (5).

Carcinogenesis undergoes multistage progression owing to accumulation of genetic and epigenetic alterations, mutations, and signaling molecules that control critical aspects of cell biology (6, 7). Changes in genetic can

be ascribed to the occurrence of proto-oncogenes and anti-oncogenes errors that initiate and drive cancer progression (8). Transmembrane protein 40 (TMEM40), a member of the TMEM family, encodes a multi-pass membrane protein, which is placed on chromosome segment 3p25.2 (9). Yu *et al.* (10) revealed that TMEM40 is located in the arthritis-related genomic regions of mouse, rat, and human, and may be associated with arthritis in these three species through the use of QTL mapping technology. In comparison with frontotemporal lobar degeneration and asymptomatic carriers, patients carrying Granulin (GRN) mutations exhibited higher levels of TMEM40 (11). Recently, TMEM40 has been reported to be associated with bladder cancer clinicopathological parameters, malignant behavior and metastasis (12). Moreover, previous report revealed TMEM members could be regulated by miRNA molecules as critical regulators for cell development

and function (13). For instance, TMEM59, the target of miR-351 in human nervous system, is essential for neural stem cell morphogenesis (14).

In recent years, microRNAs (miRNAs), a group of short non-coding RNAs (~22 nt), have attracted considerable attention due to their potential role in almost all multi-organism processes including mammals (15). Because of their inversely regulate hundreds of target genes, they have pivotal roles in proliferation, cell fate, and differentiation (15). In 1993, Lee *et al.* (16) provided the first miRNA, *lin-4*, in *Caenorhabditis elegans*. Interestingly, the functional correlation between miRNA and human cancer was preliminarily revealed by Calin *et al.* (17) that frequently loss of miR-15 and miR-16 are observed in chronic lymphocytic leukemia. After that, accumulating studies identified a large number of miRNAs role as onco-miRs or anti-onco-miRs in human cancer (18). MiR-138-5p, belonging to the miRNAs family, is a recently emerged tumor suppressor in bladder cancer (19), pancreatic cancer (20), colorectal cancer (21), and non-small cell lung cancer (22). Previous studies have suggested that the involvement of miR-138-3p in the tumorigenesis and development of these types of cancers through binding to the 3'UTR miRNA recognition elements of their target mRNAs. However, the biological role of miR-138-3p in ccRCC remains to be illuminated.

Our preliminary investigation revealed a number of genes as the potential targets for miR-138-5p by using bioinformatics, among which, TMEM40 came to our attention due to its role in bladder cancer. In the current study, quantitative real-time PCR, colony formation, invasion, migration, luciferase reporter assay, as well as clinico-pathological features were performed to ascertain miR-138-5p in ccRCC cells behaviors and its interaction with TMEM40. Our study may provide important clues with regards to prognostic, diagnostic, and management of the ccRCC.

2. Objectives

According to the association of TMEM40 and miR-138-5p with tumorigenesis, we aimed to investigate the biological function of TMEM40 and miR-138-5p in ccRCC, as well as their targeted regulation in ccRCC.

3. Materials and Methods

3.1. Patients and Tissue Samples

Surgically excised paired tumor tissues and the adjacent non-tumor kidney tissues were collected from 36 ccRCC patients after clinical and pathological confirmations in the Department of Urology, Xiangyang Central Hospital.

All ccRCC cases were staged based on the 2011 Union for International Cancer Control TNM classification of malignant tumors. These patients didn't receive chemotherapy or radiotherapy prior to surgery. The clinical characteristics of the enrolled patients are shown in **Table 1**. All tissue samples were preserved with flash freezing in liquid nitrogen after resection and stored at -80°C until quantitative real-time and Western blot analysis. Written informed consent was obtained from all patients and the study was approved by the Institutional Review Board of Xiangyang Central Hospital.

Table 1. Clinicopathological features in clear cell Cases cell carcinoma patients

Characteristics	Number of Cases (n = 36)
Age	
≤ 65	24
> 65	12
Gender	
Male	17
Female	19
TNM stage	
I	12
II	8
III	9
IV	7
Lymph node metastasis	
Yes	10
No	26

3.2. RNA Extraction and Quantitative Real-Time PCR

Total RNA was extracted from tissue samples or cultured cells with TRIzol standard protocol (Invitrogen, USA). For the detection of miR-138-5p expression, the cDNA was synthesized from 1 μg total RNA using the miScript Reverse Transcription kit (Qiagen) after purification with the RNeasy Maxi kit (Qiagen). Next, real-time PCR was performed in triplicate on the ABI 7500 fast real-time PCR System (Applied Biosystems, USA) using a Taq Man miRNA assay according to the manufacture's instruction (Applied Biosystems, CA, USA). U6 was used as an internal control for miR-138-5p calculation. To quantify TMEM40 mRNA expression, 1 μg of total RNA was reverse transcribed into cDNA using PrimeScript RT reagent Kit (Takara, Dalian, China). The real-time PCR was performed in triplicate on the ABI 7500 fast real-time PCR System (Applied Biosystems, USA) using SYBR Green PCR

kit (Takara, Dalian, China) following the manufacturer's instruction. GAPDH was used as an internal control for detection of TMEM40 mRNA. The primer sequences were listed as follows: miR-138-5p primers: (Forward, 5'-CGCGATGTGTAAACATCCTCGAC-3'; Reverse, 5'-ATCCAGTGCAGGGTCCGAGG-3'); U6 primers: (Forward, 5'-CTCGCTTCCGGCAGCACA-3'; Reverse, 5'-ACGCTTACGAATTTGCGT-3'); TMEM40 primers: (Forward, 5'-GCGGTAGGGGTGTACGGT-3'; Reverse, 5'-CCGGACACGCTGAACCTTGT-3'); GAPDH primers: (Forward, 5'-CGCTCTCTGCTCCTCCTGTTC-3'; Reverse, 5'-ATCCGTTGACTCCGACCTTAC-3'). The relative levels of miR-138-5p or TMEM40 mRNA were calculated using the comparative $2^{-\Delta\Delta C_t}$ method.

3.3. Protein Extraction and Western blot

The tissues specimens or cells were lysed in ice-cold RIPA lysis buffer (Beyotime, Shanghai, China) and then incubated for 30 min on ice. After centrifuged for 15 min at 4 °C, the supernatant was collected and the concentration of total protein was determined by BCA protein assay kit (Beyotime, Shanghai, China). Equal amounts of the total protein of the tissues or cells were separated on 10% SDS-PAGE and then transferred onto polyvinylidene fluoride membrane (Millipore, Boston, MA, USA). The membrane was blocked in 5% non-fat milk, and then incubated with rabbit anti-TMEM40 (ab126386, Abcam, USA) or GAPDH (Cell Signaling Technology, USA). After washing, the membrane was incubated with the goat anti-rabbit IgG HRP (ab205718, Abcam, USA). The protein signal intensity was detected with ECL chemiluminescent kit (Thermo Fisher Scientific). The final results were expressed as the fold changes by normalizing the protein levels to the GAPDH values.

3.4. Cell Culture

The human ccRCC cell lines, 786-O, ACHN cells and human embryonic kidney 293T cells were purchased from the cell bank of the Chinese Academy of Sciences (Shanghai, China). 786-O cells were cultured in RPMI-1640 medium (HyClone) with 10% FBS (Gibco). ACHN and 293T cells were cultured in DMEM medium (Gibco) supplemented with 10% fetal bovine serum (Gibco). All cell lines were maintained at 37 °C in a humidified incubator containing 5% CO₂.

3.5. MicroRNA, siRNA and Plasmid Transfection

MiR-138-5p mimics (miR-138-5p: 5'-AGCUGGUGUUGUGAAUCAGGCCG-3'), negative control miRNA (miR-NC: 5'-ACTACTGAGTGACAGTAGA-3'), TMEM40 siRNA

(siTMEM40: 5'-GGAUGAGCUUCAACUCUAUTT-3') and siNC (5'-UUCUCCGAACGUGUCACGUTT-3') were synthesized by Shanghai GenePharma Company. For cell transfection, 786-O and ACHN cells were seeded into 6-well plates until reached 60-70% confluency. MiR-138-5p overexpression was achieved by transfecting with miR-138-5p (50 nM) for 48 h, and TMEM40 knockdown was achieved by transfecting with siTMEM40 (50 nM) for 48 h. All cell transfections were performed using Lipofectamine 2000 reagent (Invitrogen, USA) following the manufacturer's instructions.

3.6. Cell Proliferation Assay

The proliferative ability of 786-O and ACHN cells was determined using the Cell Counting Kit-8 (CCK-8, Dojindo) according to the manufacturer's instructions. In brief, transfected 786-O and ACHN cells were seeded in 96-well plates at a density of 5×10^3 cells per well. At 0, 24, 48, and 72 h after seeding, 10 μ L of CCK-8 reagent was added to each well and the cells were continually incubated for 2 h in a humidified incubator containing 5% CO₂. The optical density (OD) value was measured at a wavelength of 450 nm using an ELISA microplate reader (Bio Rad Laboratories, CA, USA). Five replicates of each sample were prepared and run five times.

3.7. Colony Formation Assay

For colony formation assay, ACHN cells were plated in 6-well plates at a density of 500 cells per well and incubated for 7 days. Subsequently, cells were fixed with ice-cold methanol for 30 min at room temperature and then stained with 1% crystal violet. The number of colonies (more than 50 cells per colony) was counted under a light microscope (Olympus, Tokyo, Japan).

3.8. Wound Healing Assay

Cell migration ability of 786-O and ACHN cells was estimated using a wound-healing assay. Briefly, transfected cells were seeded onto 6-well plates (4×10^5 cells/well). After 24 h incubation, a sterile tip of 200 μ L pipette was assigned to scratch monolayer of cells to make a wound field in each well. Subsequently, a light microscope (Leica Microsystems) was used to observe and capture representative images at 0 h and 48 h after scouring. The relative distance of migrating cells from five different areas was calculated as an assessment for the wound healing rate.

3.9. Transwell Assay

Transwell assay was performed to evaluate the invasion ability of the 786-O and ACHN cells after transfection. In the invasion assay, BD Matrigel (BD Biosciences,

CA, USA) was added to the upper chamber of the 24-well Transwell chamber with 8.0 μm pore size (Costar, USA). Subsequently, a total of 2×10^4 transfected cells in serum-free medium were seeded into the upper chamber. A total 500 μL medium with 10% FBS was added into the lower chambers as a chemoattractant. After 48 h incubation at 37 °C, all the invaded cells on the lower surface were fixed with formalin and stained with 0.1% crystal violet for 5 min. The number of invaded cells was counted under a light microscope in five randomly selected fields and the average value was calculated.

3.10. Prediction of Target Genes of miR-138-5p

The miRNA target predicting algorithms TargetScan Release 7.1 (http://www.targetscan.org/vert_71/), starBase v2.0 (<http://starbase.sysu.edu.cn/>) were used to predict the direct targets of miR-138-5p and their binding regions.

3.11. Dual Luciferase Activity Assay

The relationship between miR-138-5p and TMEM40 was further confirmed using dual luciferase reporter assay. In brief, the wild-type (Wt) TMEM40-3'UTR was cloned into the psi-CHECK-2 vector (Promega, USA) at XhoI and EcoRI restriction sites. TaKaRa Mutan BEST Kit (Takara, Japan) was used to chemically synthesize the mutant (Mut) TMEM40-3'UTR containing the putative binding site of miR-138-5p. Afterwards, 293T cells were seeded into 24-well plates and grew until 80% confluence. Cells were then co-transfected with 0.5 μg of constructed reporter plasmid (Wt TMEM40 3'UTR or Mut TMEM40 3'UTR) together with miR-138-5p or control miR-NC at a final concentration of 50 nM. After 48 h transfection, dual luciferase reporter assay was performed with a Dual-Luciferase Reporter Assay System (Promega) according to the manufacturer's instructions.

3.12. Statistical Analysis

Statistical analysis was performed using SPSS 17.0 (IBM Corporation, Armonk, NY, USA). All quantitative data are expressed as the mean \pm standard deviation (SD) from at least three separate experiments. Pearson's correlation coefficient was utilized to evaluate the correlation between miR-138-5p and TMEM40 expression in ccRCC tissues by GraphPad Prism 6.0 software. Student's paired two-tailed *t*-test or ANOVA, or One-way ANOVA with Bonferroni post-hoc tests was applied, where appropriate. A probability of $p < 0.05$ was considered significant.

4. Results

4.1. Reverse Correlation between miR-138-5p and TMEM40 in ccRCC Tissue Specimens

To explore whether miR-138-5p functionally regulate the expression of TMEM40, we examined the expression of miR-138-5p and TMEM40 in ccRCC tumor tissues. As shown in **Figure 1A**, the expression of miR-138-5p was significantly down-regulated in 36 pairs of ccRCC tissues in comparison with adjacent normal tissues ($p < 0.001$). On the contrary, relatively higher amounts of TMEM40 mRNA were detected in these tumor tissues (**Fig. 1B**, $p < 0.001$). Subsequently, we analyzed the correlation between miR-138-5p and TMEM40 in ccRCC tissues based on their mRNA levels. As presented in **Figure 1C**, the expression of miR-138-5p was reversely associated with the TMEM40 mRNA to a significant level in ccRCC tissues ($p = 0.0405$). In addition, the protein levels of TMEM40 were determined using Western blot. As shown in Figure 1D and E, a significant increased level of TMEM40 expression was observed in the 8 representative pairs of ccRCC tissues compared to the corresponding noncancerous tissues ($p = 0.0144$). These results provide strong evidence to support that hypothesis that there was reverse correlation between miR-138-5p and TMEM40 in ccRCC tissue.

4.2. Inhibitory Effects of miR-138-5p Overexpression or TMEM40 Knockdown on ccRCC Cell Proliferation

To elucidate the biological functions of miR-138-5p or TMEM40 in ccRCC *in vitro*, 786-O and ACHN cells were transfected with miR-138-5p mimics to acquire miR-138-5p overexpressing cell lines or siTMEM40 to obtain TMEM40 knockdown cell lines. The CCK-8 assay was first used to measure cell proliferative ability in 786-O and ACHN cells. The results showed that the proliferation of 786-O (**Figure 2A**, $p < 0.001$) and ACHN cells (**Fig. 2B**, $p < 0.001$) was significantly reduced after transfection with miR-138-5p compared with miR-NC. Similar results were also observed in 786-O (**Fig. 2C**, $p < 0.001$) and ACHN cells (**Figure 2D**, $p < 0.001$) after transfection with siTMEM40. Furthermore, colony formation assay was performed in ACHN cells. Consistently, overexpression of miR-138-5p (**Fig. 2E**, $p < 0.001$) or TMEM40 knockdown (**Fig. 2F**, $p < 0.001$) remarkably suppressed colony formation ability in ACHN cells. These results indicated existence of opposite effects of miR-138-5p and TMEM40 in the regulation of ccRCC cell proliferation.

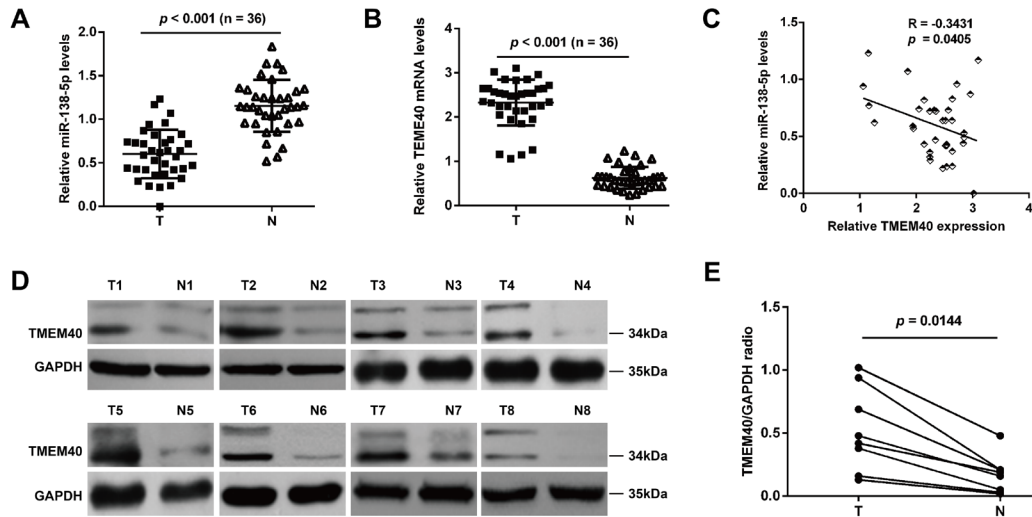


Fig 1. miR-138-5p and TMEM40 expression levels are negatively correlated in ccRCC patient tissues samples. Quantitative real-time PCR analysis for (A) miR-138-5p and (B) TMEM40 in 36 paired ccRCC and adjacent normal tissues. (C) The Pearson's correlation analysis for the relationship between miR-138-5p levels and TMEM40 mRNA levels in ccRCC tissues. (D and E) Western blot analysis for TMEM40 expression in 8 paired ccRCC and adjacent normal tissues. T1-8 presents tumor tissues and N1-8 presents paired normal tissues.

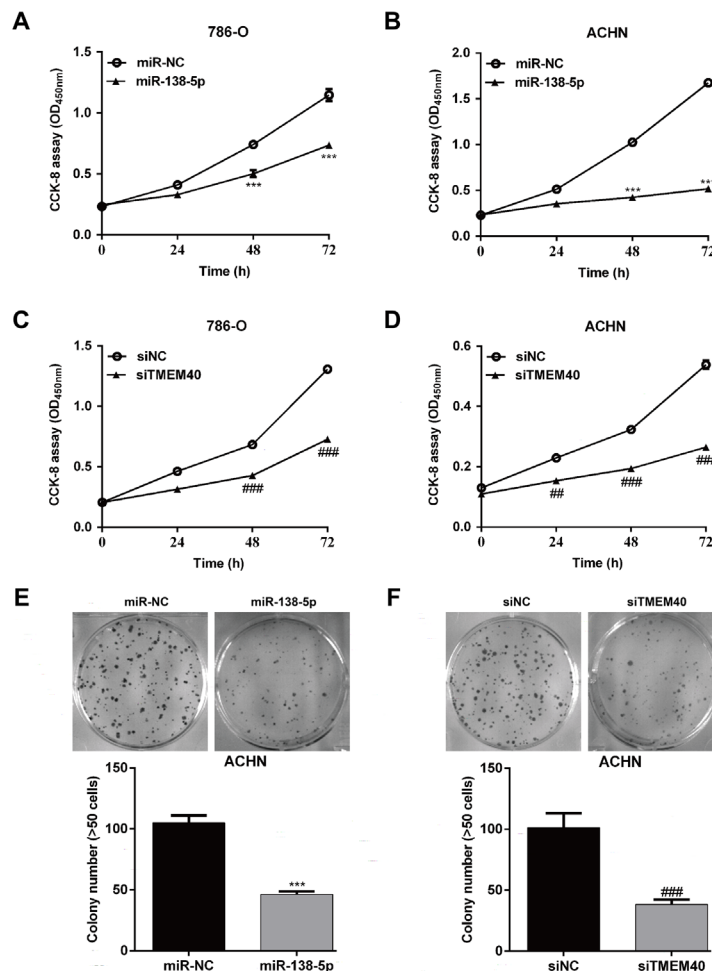


Fig 2. The ability of miR-138-5p and TMEM40 in cell proliferation was assessed by CCK-8 assay. (A) 786-O cells and (B) ACHN cells were transfected with miR-138-5p mimic or miR-NC and underwent CCK-8 assay. (C) 786-O cells and (D) ACHN cells were transfected with siTMEM40 or siNC and underwent CCK-8 assay. Colony formation was measured in ACHN cells transfected with (E) miR-138-5p mimic or transfected with (F) siTMEM40. *** $p < 0.001$, compared with miR-NC; ### $p < 0.01$, #### $p < 0.001$, compared with siNC; NC, negative control; OD, optical density; CCK8, Cell Counting Kit 8

4.3. Inhibitory Effects of miR-138-5p Overexpression or TMEM40 Knockdown on ccRCC Cell Migration and Invasion

Next, the ability of miR-138-5p or TMEM40 on cell mobility was assessed by wound healing assay and

transwell assay. In wound-healing assay (**Fig. 3**), the wound healing rate of 786-O and ACHN cells in the group transfected with miR-138-5p mimics were significantly lower than miR-NC after 48 h culture.

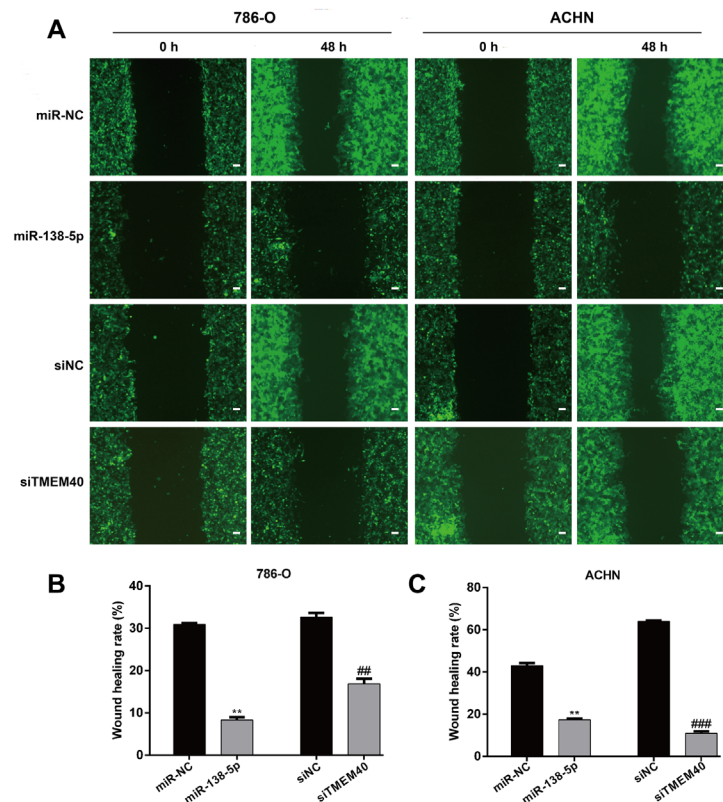


Figure 3. The ability of miR-138-5p and TMEM40 in cell migration was assessed by wound healing assay. (A) Representative cell migratory distances images in 786-O and ACHN cell lines. Statistical analysis of wound healing rate in (B) 786-O and (C) ACHN cells after transfection with miR-138-5p mimic or miR-NC and siTMEM40 or siNC; ** $p < 0.01$, compared with miR-NC; ## $p < 0.01$, ### $p < 0.001$, compared with siNC; NC, negative control

Similarly, the wound healing rate of 786-O and ACHN cells in the group transfected with siTMEM40 were remarkably decreased compared with siNC. In the transwell assay (**Fig. 4**), miR-138-5p overexpression significantly suppressed the invasive cell number in 786-O cells by 57.17% (miR-NC vs. miR-138-5p, 120.7 ± 8.1 vs. 51.7 ± 7.4 , $p < 0.01$) and ACHN cells by 81.84% (miR-NC vs. miR-138-5p, 103.0 ± 4.4 vs. 18.7 ± 3.1 , $p < 0.001$). Consistently, TMEM40 knockdown inhibited invasive cell number in 786-O cells by 67.23% (siNC vs. siTMEM40, 130.3 ± 3.2 vs. 42.7 ± 1.5 , $p < 0.01$) and ACHN cells by 74.80% (siNC vs. siTMEM40, 127.0 ± 7.5 vs. 32.0 ± 1.0 , $p < 0.01$). These data further demonstrated that miR-138-5p exerted inhibitory effects, while TMEM40 presented facilitating function on the ccRCC cell mobility.

4.4. Validation of TMEM40 as a Direct Target of miR-138-5p in ccRCC Cells

To clarify whether miR-138-5p could directly interact

with TMEM40 in ccRCC cells, we used the public database to search for the potentially downstream targets of miR-138-5p. As expected, we found that the 3'-UTR of TMEM40 contained the complementary sequences for miR-138-5p binding site (**Fig. 5A**). To validate miR-138-5p could indeed bind to the 3'-UTR of TMEM40, we performed luciferase activity assay for Wt TMEM40 3'-UTR and Mut TMEM40 3'-UTR. The results demonstrated that miR-138-5p overexpression significantly decreased the luciferase activity of Wt TMEM40 3'-UTR, but did not have any effect on the luciferase activity of Mut TMEM40 3'-UTR (Figure 5B, $p < 0.01$). Furthermore, quantitative real-time PCR and Western blot confirmed that miR-138-5p overexpression decreased the mRNA and protein level of TMEM40 in 786-O (**Fig. 5C and D**, $p < 0.001$) and ACHN cells (**Fig. 5E and F**, $p < 0.001$).

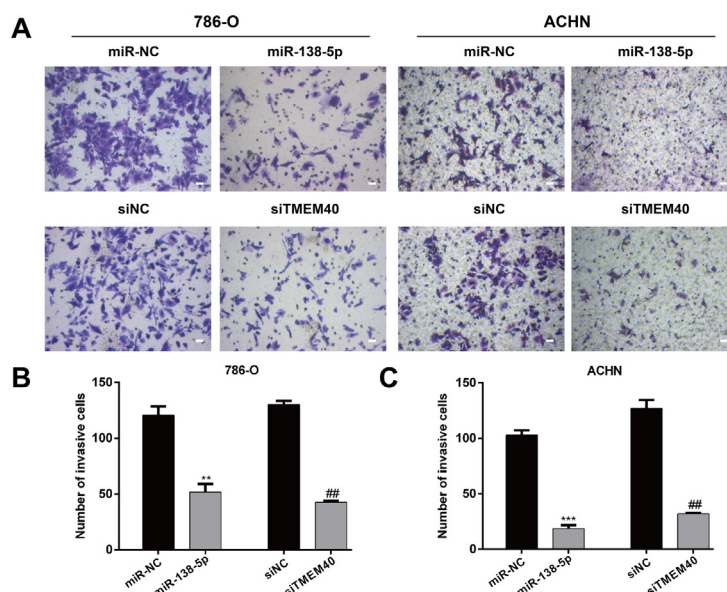


Fig 4. The ability of miR-138-5p and TMEM40 in cell invasion was assessed by transwell assay. (A) Representative cell invasive images in 786-O and ACHN cell lines. Statistical analysis of invasive cell number in (B) 786-O and (C) ACHN cells after transfection with miR-138-5p mimic or miR-NC and siTMEM40 or siNC; ** $p < 0.01$, *** $p < 0.001$, compared with miR-NC; ### $p < 0.01$, compared with siNC; NC, negative control

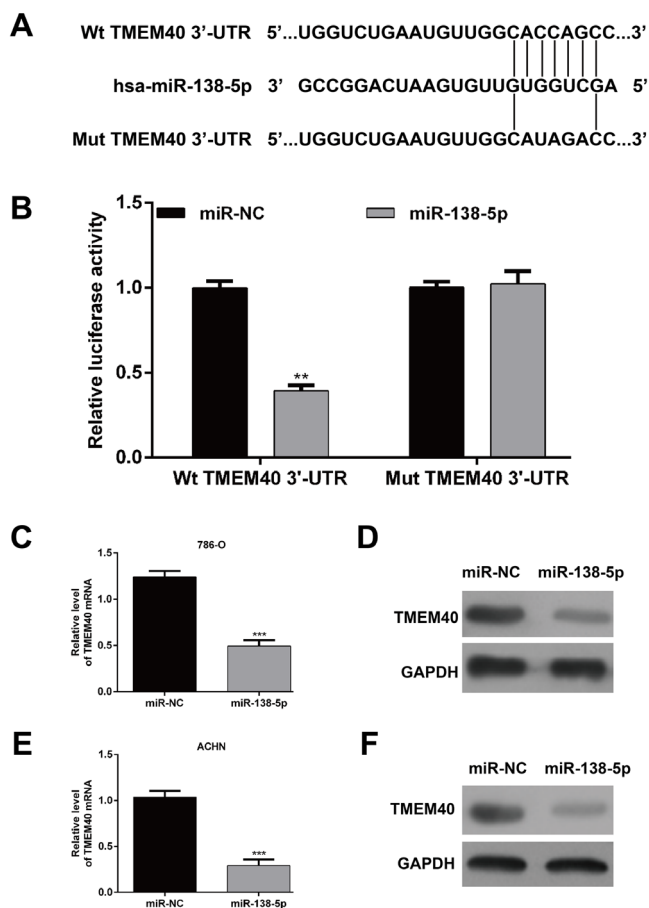


Fig 5. TMEM40 was the downstream target of miR-138-5p in ccRCC. (A) miR-138-5p and its putative binding sequence in the 3'-UTR of TMEM40. Mutated TMEM40 3'-UTR was generated in the complementary site for the seed region of miR-138-5p. (B) miR-138-5p overexpression significantly suppressed the luciferase activity of wild type TMEM40 3'-UTR but not mutated 3'-UTR of TMEM40. (C) The mRNA level of TMEM40 and (D) the protein level of TMEM40 were significantly inhibited in 786-O cells after miR-138-5p overexpression. (E) The mRNA level of TMEM40 and (F) the protein level of TMEM40 were significantly suppressed in ACHN cells after miR-138-5p overexpression. ** $p < 0.01$, *** $p < 0.001$, compared with miR-NC; NC, negative control

5. Discussion

Accumulating evidence point an important role for miRNAs in the modulation of cancer progression and is associated with carcinogenesis and development (23). It is well known that multiple oncogenes and anti-oncogenes can be targeted by miRNAs in a cell type-specific manner (24). Therefore, determination of differentially expressed miRNAs and their target gene networks is of great help in understanding the pathological mechanism in ccRCC. MiR-138-5p is a tumor suppressor that inhibits colorectal cancer cells and S-phase entry through targeting PD-L1 (21). In non-small lung cancer cells, miR-138-5p is reported to reverse the gefitinib resistance via downregulation of G-protein-coupled receptor 124 (22). Besides, a strong correlation between miR-138-5p and SIRT1 and FOXC1 are respectively noted in the intervertebral disc degeneration (IDD) and pancreatic cancer (20, 25). However, few studies have supplied evidence for a relationship between miR-138-5p expression patterns and ccRCC malignant behavior.

Here, we reported that miR-138-5p was remarkably decreased in the patients' tissues with ccRCC compared to the adjacent normal tissues. What's more, TMEM40 as a novel target for miR-138-5p. In a further, both ectopic expression of miR-138-5p and knockdown of TMEM40 in ccRCC 786-O and ACHN caused inhibition of cells proliferation, migration, and invasion. Our reports provide a molecular explanation that enhanced expression of miR-138-5p at least partially decreased proliferation, migration and invasion through directly targeting TMEM40 in ccRCC cells.

As a hallmark of cancer, uncontrolled cellular proliferation is driven by alteration of a restricted number of critical pathways (26, 27). For example, deficiency of retinoblastoma protein, inadequate formation of CDK4/6-Cyclin D1 complexes or hyperactivation of these complexes could decrease the sensitivity of tumor cells to requirement of mitogenic signaling, leading to promotion of cell proliferation (28). Upregulation of CDK2 and downregulation of p27Kip1 are responsible for promotion of haematopoietic cell proliferation induced by BCR-ABL (29). More importantly, loss of TMEM40 could relieve the enhanced bladder cancer cell proliferation via the changed expression levels of p53, p21, c-MYC, and cyclin D1. We hypothesize that the proliferation-related signals, especially for cell cycle progression, possibly decreased the proliferation of miR-138-5p-overexpressed cells through targeting TMEM40.

Metastasis is a multiple-step process implicating migration and invasion of primary tumor cells which will subsequently reaches at a secondary location (30).

It is well known that invasion and migration are the two most life-threatening aspects of human cancers, including ccRCC (31). A widely varying mechanisms in cancer cells has been shown to be closely related to the occurrence of the metastasis (31). Previous studies have identified integrin activity, focal-contact formation, and actomyosin-dependent contractility are mediators of cancer-cell motility (32). The aggressive types of human cancers frequently exhibit elevated levels of ECM-degrading enzymes, like matrix metalloproteinases and cathepsins (31). Besides, activation of RAC, RHO, ROCK, and/or MLCK signaling events are important factors in the migration, invasion and development in diverse malignancies (31, 33). Recently, miR-22, miR-29s, and miR-124 are correlated with ccRCC invasion and migration, and miR-138-5p is deemed as one of the tumor suppressors in multiple types of cancer (34-36). In the current study, we characterized the miR-138-5p mimics and siTMEM40 ccRCC cell lines 786-O and ACHN possessed a weak invasive and migratory activity compared to the control, indicating that targeted disruption of the TMEM40 gene in ccRCC cells could greatly reduce cancer cell mobility ability.

6. Conclusion

In conclusion, the outcomes of the present study uncovered that miR-138-5p is significantly decreased in ccRCC tissues and negatively correlated with TMEM40. Enhanced expression of miR-138-5p has inhibitory actions on the multiple malignant biological behaviors through down-regulating TMEM40. Although further research efforts need to explore the mechanisms underlying miR-138-5p regulating proliferation, invasion and migration of ccRCC cells, the miR-138-5p-TMEM40 interaction may provide an important clue for ccRCC diagnosis, prognosis, and management.

Competing interests

The authors declare that they have no competing interests.

References

1. Brugarolas J. Molecular genetics of clear-cell renal cell carcinoma. *J Clin Oncol.* 2014;**32**(18):1968-1976.doi:10.1200/JCO.2012.45.2003
2. Kostrzewa M, Zyla M, Wladzinski J, Stetkiewicz T, Stachowiak G, Wilczynski JR. Metastases of renal clear cell carcinoma to ovary--case report and review of the literature. *Eur J Gynaecol Oncol.* 2015;**36**(2):219-222
3. Baldewijns MM, van Vlodrop IJ, Schouten LJ, Soetekouw PM, de Bruine AP, van Engeland M. Genetics and epigenetics of renal cell cancer. *Biochim Biophys Acta.* 2008;**1785**(2):133-155.doi:10.1016/j.bbcan.2007.12.002
4. Petejova N, Martinek A. Renal cell carcinoma: Review of etiology, pathophysiology and risk factors. *Biomed Pap Med Fac Univ Palacky Olomouc Czech Repub.* 2016;**160**(2):183-

- 194.doi:10.5507/bp.2015.050
5. Ljungberg B, Bensalah K, Canfield S, Dabestani S, Hofmann F, Hora M, et al. EAU guidelines on renal cell carcinoma: 2014 update. *Eur Urol*. 2015;**67**(5):913-924.doi:10.1016/j.eururo.2015.01.005
 6. Jones PA, Issa JP, Baylin S. Targeting the cancer epigenome for therapy. *Nat Rev Genet*. 2016;**17**(10):630-641.doi:10.1038/nrg.2016.93
 7. Kanda M, Sugimoto H, Kodera Y. Genetic and epigenetic aspects of initiation and progression of hepatocellular carcinoma. *World J Gastroenterol*. 2015;**21**(37):10584-10597.doi:10.3748/wjg.v21.i37.10584
 8. Izumchenko E, Chang X, Brait M, Fertig E, Kagohara LT, Bedi A, et al. Targeted sequencing reveals clonal genetic changes in the progression of early lung neoplasms and paired circulating DNA. *Nat Commun*. 2015;**6**:8258.doi:10.1038/ncomms9258
 9. Rodriguez F, Vallejos C, Giraudo F, Unanue N, Hernandez MI, Godoy P, et al. Copy number variants of Ras/MAPK pathway genes in patients with isolated cryptorchidism. *Andrology*. 2017;**5**(5):923-930.doi:10.1111/andr.12390
 10. Yu X, Teng H, Marques A, Ashgari F, Ibrahim SM. High resolution mapping of Cia3: a common arthritis quantitative trait loci in different species. *J Immunol*. 2009;**182**(5):3016-3023. doi:10.4049/jimmunol.0803005
 11. Milanesi E, Bonvicini C, Alberici A, Pilotto A, Cattane N, Premi E, et al. Molecular signature of disease onset in granulysin mutation carriers: a gene expression analysis study. *Neurobiol Aging*. 2013;**34**(7):1837-1845.doi:10.1016/j.neurobiolaging.2012.11.016
 12. Zhang QY, Fu MT, Zhang ZF, Feng YZ, Wei M, Zhou JY, et al. Expression of TMEM40 in bladder cancer and its correlation with clinicopathological parameters. *Int J Clin Exp Pathol*. 2017;**10**(7):8050-8057
 13. Kong HX, Chen JJ, Liu W. (The role of pulmonary macrophages in the development of silicosis). *Zhonghua lao dong wei sheng zhi ye bing za zhi = Zhonghua laodong weisheng zhiyebing zazhi = Chinese journal of industrial hygiene and occupational diseases*. 2012;**30**(4):318-20
 14. Xu H, Yang F, Sun Y, Yuan Y, Cheng H, Wei Z, et al. A new antifibrotic target of Ac-SDKP: inhibition of myofibroblast differentiation in rat lung with silicosis. *PLoS One*. 2012;**7**(7):e40301.doi:10.1371/journal.pone.0040301
 15. Esquela-Kerscher A, Slack FJ. Oncomirs - microRNAs with a role in cancer. *Nat Rev Cancer*. 2006;**6**(4):259-269.doi:10.1038/nrc1840
 16. Lee RC, Feinbaum RL, Ambros V. The *C. elegans* heterochronic gene *lin-4* encodes small RNAs with antisense complementarity to *lin-14*. *Cell*. 1993;**75**(5):843-854
 17. Calin GA, Dumitru CD, Shimizu M, Bichi R, Zupo S, Noch E, et al. Frequent deletions and down-regulation of micro-RNA genes miR15 and miR16 at 13q14 in chronic lymphocytic leukemia. *Proc Natl Acad Sci U S A*. 2002;**99**(24):15524-15529.doi:10.1073/pnas.242606799
 18. Ohtsuka M, Ling H, Doki Y, Mori M, Calin GA. MicroRNA Processing and Human Cancer. *J Clin Med*. 2015;**4**(8):1651-1667.doi:10.3390/jcm4081651
 19. Yang R, Liu M, Liang H, Guo S, Guo X, Yuan M, et al. miR-138-5p contributes to cell proliferation and invasion by targeting Survivin in bladder cancer cells. *Mol cancer*. 2016;**15**(1):82. doi:10.1186/s12943-016-0569-4
 20. Yu C, Wang M, Li Z, Xiao J, Peng F, Guo X, et al. MicroRNA-138-5p regulates pancreatic cancer cell growth through targeting FOXC1. *Cell Oncol (Dordr)*. 2015;**38**(3):173-181.doi:10.1007/s13402-014-0200-x
 21. Zhao L, Yu H, Yi S, Peng X, Su P, Xiao Z, et al. The tumor suppressor miR-138-5p targets PD-L1 in colorectal cancer. *Oncotarget*. 2016;**7**(29):45370-45384.doi:10.18632/oncotarget.9659
 22. Gao Y, Fan X, Li W, Ping W, Deng Y, Fu X. miR-138-5p reverses gefitinib resistance in non-small cell lung cancer cells via negatively regulating G protein-coupled receptor 124. *Biochem Biophys Res Commun*. 2014;**446**(1):179-186.doi:10.1016/j.bbrc.2014.02.073
 23. Pereira DM, Rodrigues PM, Borralho PM, Rodrigues CM. Delivering the promise of miRNA cancer therapeutics. *Drug Discov Today*. 2013;**18**(5-6):282-289.doi:10.1016/j.drudis.2012.10.002
 24. Bertoli G, Cava C, Castiglioni I. MicroRNAs: New Biomarkers for Diagnosis, Prognosis, Therapy Prediction and Therapeutic Tools for Breast Cancer. *Theranostics*. 2015;**5**(10):1122-1143. doi:10.7150/thno.11543
 25. Wang B, Wang D, Yan T, Yuan H. MiR-138-5p promotes TNF-alpha-induced apoptosis in human intervertebral disc degeneration by targeting SIRT1 through PTEN/PI3K/Akt signaling. *Exp Cell Res*. 2016;**345**(2):199-205.doi:10.1016/j.yexcr.2016.05.011
 26. Cantor JR, Sabatini DM. Cancer cell metabolism: one hallmark, many faces. *Cancer Discov*. 2012;**2**(10):881-898. doi:10.1158/2159-8290.CD-12-0345
 27. Evan GI, Vousden KH. Proliferation, cell cycle and apoptosis in cancer. *Nature*. 2001;**411**(6835):342-348.doi:10.1038/35077213
 28. Deshpande A, Sicinski P, Hinds PW. Cyclins and cdks in development and cancer: a perspective. *Oncogene*. 2005;**24**(17):2909-2915.doi:10.1038/sj.onc.1208618
 29. Parada Y, Banerji L, Glassford J, Lea NC, Collado M, Rivas C, et al. BCR-ABL and interleukin 3 promote haematopoietic cell proliferation and survival through modulation of cyclin D2 and p27Kip1 expression. *J Biol Chem*. 2001;**276**(26):23572-23580. doi:10.1074/jbc.M101885200
 30. Bhatia M, McGrath KL, Di Trapani G, Charoentong P, Shah F, King MM, et al. The thioredoxin system in breast cancer cell invasion and migration. *Redox Biol*. 2016;**8**:68-78. doi:10.1016/j.redox.2015.12.004
 31. Friedl P, Wolf K. Tumour-cell invasion and migration: diversity and escape mechanisms. *Nat Rev Cancer*. 2003;**3**(5):362-374. doi:10.1038/nrc1075
 32. Gimona M, Buccione R. Adhesions that mediate invasion. *Int J Biochem Cell Biol*. 2006;**38**(11):1875-1892.doi:https://doi.org/10.1016/j.biocel.2006.05.003
 33. Avizienyte E, Frame MC. Src and FAK signalling controls adhesion fate and the epithelial-to-mesenchymal transition. *Curr Opin Cell Biol*. 2005;**17**(5):542-547.doi:10.1016/j.ceb.2005.08.007
 34. Fan W, Huang J, Xiao H, Liang Z. MicroRNA-22 is downregulated in clear cell renal cell carcinoma, and inhibits cell growth, migration and invasion by targeting PTEN. *Mol Med Rep*. 2016;**13**(6):4800-4806.doi:10.3892/mmr.2016.5101
 35. Nishikawa R, Chiyomaru T, Enokida H, Inoguchi S, Ishihara T, Matsushita R, et al. Tumour-suppressive microRNA-29s directly regulate LOXL2 expression and inhibit cancer cell migration and invasion in renal cell carcinoma. *FEBS Lett*. 2015;**589**(16):2136-2145.doi:10.1016/j.febslet.2015.06.005
 36. Butz H, Szabo PM, Khella HW, Nofech-Mozes R, Patocs A, Yousef GM. miRNA-target network reveals miR-124as a key miRNA contributing to clear cell renal cell carcinoma aggressive behaviour by targeting CAV1 and FLOT1. *Oncotarget*. 2015;**6**(14):12543-12557.doi:10.18632/oncotarget.3815